ELSEVIER

Catalysis Today 68 (2001) 69–74

CATALYSIS TODAY

www.elsevier.com/locate/cattod

Coexistence of paramagnetic and superparamagnetic Fe(III) in mesoporous MCM-41 silicates

P. Selvam [a,*], S.E. Dapurkar [a], S.K. Badamali [a], M. Murugasan [b], H. Kuwano [b]

[a] *Department of Chemistry, Indian Institute of Technology – Bombay, Powai, Mumbai 400 076, India*
[b] *Department of Material Science and Engineering, Muroran Institute of Technology, Muroran 050 0071, Japan*

This paper is dedicated to Prof. B. Viswanathan on the occasion of his 60th birthday

Abstract

In the present study, we demonstrate the coexistence of paramagnetic and superparamagnetic Fe(III) in mesoporous MCM-41 matrix. The loading of trivalent iron in MCM-41 not only results in the formation of iron oxide nanoclusters in the mesovoids, but also substitutes (isomorphously) in the silicate matrix. The resulting non-framework and framework Fe(III) exhibit superparamagnetic and paramagnetic properties, respectively. The dual behaviour of Fe(III) in MCM-41 is deduced using various analytical and spectroscopic techniques, viz. X-ray diffraction (XRD), diffuse reflectance ultraviolet–visible (DRUV–VIS), electron paramagnetic resonance (EPR) and Mössbauer spectroscopy.

Keywords: MCM-41; Mesoporous molecular sieves; Iron oxide nanoclusters; Paramagnetism; Superparamagnetism

1. Introduction

In recent years, nanosized materials have received significant attention due to their outstanding physicochemical properties. Several diverse applications of these materials, e.g. high density magnetic recording, magnetic fluids, colours imaging, magnetic refrigeration as well as in photocatalysis, nonlinear optics, solar cells, photosensors and light emitting diodes, have triggered considerable research activities in the area of nanotechnology [1–4]. Furthermore, nanoscale magnetic particles exhibit a remarkable physical phenomenon, viz. superparmagnetism [5]. Another well-known cluster related concept is the so-called quantum size effect, which arises as a result of the (blue) shift in the optical absorption edge of nanoparticles [6]. Nevertheless, from a viewpoint of nanoclusters in confined environment, e.g. micropores of certain molecular sieves (zeolites), only little effort has been directed. The well-defined and regular pore structure of zeolites [7,8] offer an unique microenvironment for the confinement of nanosized materials [9–11], however, the much smaller pore sizes of these materials limit their applicability as molecular hosts.

On the other hand, the discovery [12,13] of M41S family of mesoporous solids, in the early 1990s, has revolutionised research in many areas of science and technology including nanomaterials [14–17]. The hexagonal and cubic members of the family, viz. MCM-41 and MCM-48, have been considered as ideal hosts for a number of potential guest molecules [17,18]. Recently, the formation of iron oxide nanoparticles in the mesopores of MCM-41 and MCM-48 were reported [19–22]. However, the interpretation of experimental results, in particular the diffuse

* Corresponding author. Fax: +91-22-572-3480.
E-mail address: selvam@iitb.ac.in (P. Selvam).

0920-5861/01/$ – see front matter
PII: S0920-5861(01)00292-9

reflectance ultraviolet–visible data [19,20], requires an appropriate analysis owing to the possibility of Fe(III) occupying the various available sites in the silicate matrix, viz. framework, non-framework and extra framework positions [23,24]. In view of the above, we have carried out a careful investigation on the incorporation of iron oxide nanoparticles in MCM-41 in order to unravel complications involved in these systems. For comparison, ferrisilicate (FeMCM-41) was prepared hydrothermally and some spectral data were discussed. All the samples were systematically characterised using various physico-chemical methods such as X-ray diffraction (XRD), diffuse reflectance ultraviolet–visible (DRUV–VIS), electron paramagnetic resonance (EPR), Mössbauer and inductively coupled plasma-atomic emission spectroscopy (ICP-AES).

2. Experimental

2.1. Starting materials

The following materials were used for the preparation of MCM-41, FeMCM-41 and loading purposes. Fumed silica (SiO_2; 99.8%, Aldrich), tetramethylammonium hydroxide (TMAOH; 25 wt.% solution, Aldrich), cetyltrimethylammonium bromide (CTAB; 99%, Aldrich), sodium hydroxide (NaOH; Loba, 98%), Iron(III) nitrate nonahydrate ($Fe(NO_3)_3{\cdot}9H_2O$; Alfa, 98%), sulphuric acid (H_2SO_4; BDH, 98%) and distilled water. All the chemicals were used in the as-received forms without any further purification. The bulk iron oxy-hydroxide, FeO(OH) was freshly prepared as per the procedure outlined earlier [23,24]. For comparison, bulk iron oxide (Fe_2O_3; 99%, Merck) was used in the as-received form.

2.2. Synthesis of MCM-41 and FeMCM-41

Mesoporous silicate MCM-41 and ferrisilicate FeMCM-41 samples were hydrothermally synthesised in teflon-lined stainless steel autoclaves according to the procedure described elsewhere [23,24]. The samples were crystallised with a typical gel (molar) composition of $10SiO_2$:$1.35(CTA)_2O$:$0.75(TMA)_2O$:$680H_2O$, and SiO_2:$0.25(CTA)_2$:$0.25Na_2O$:$0.108H_2SO_4$:$68H_2O$:$0.005Fe_2O_3$, at 373 K for 1 day (MCM-41), and at 423 K for 9 days (FeMCM-41), respectively. The solid products obtained were washed, filtered and dried in an air oven at 353 K for 12 h. The dried samples were then calcined in a tubular furnace at 823 K in a flow of N_2 for 1 h followed by 8 h in air.

2.3. Loading of $FeO(OH)/Fe_2O_3$

The loading of $FeO(OH)/Fe_2O_3$ was carried out on well characterised calcined MCM-41 by the incipient wetness method at room temperature with 0.008 M aqueous iron nitrate at a pH < 2.0. The loaded sample, viz. FeO(OH)/MCM-41, was washed, after being kept for 6–7 h, filtered and dried at 373 K. It was then calcined at 773 K in air for 5–6 h, and the resulting sample is referred as Fe_2O_3/MCM-41.

2.4. Characterisation

Powder XRD patterns were recorded in the low angle ($2\theta = 1$–10°) region with Rigaku/Siemens diffractometers using a nickel filtered Cu Kα radiation with a wavelength of 1.5418 Å and a step size of 0.02°. DRUV–VIS spectra of the samples were recorded (200–700 nm) on an UV-260 Shimazdu spectrophotometer. EPR spectra of the samples were recorded on a varian (E-line century series E-112) spectrometer

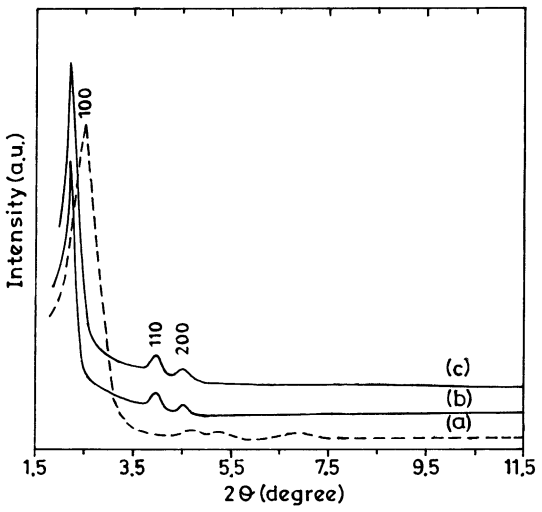

Fig. 1. XRD patterns of: (a) calcined MCM-41; (b) FeO(OH)/MCM-41; (c) Fe_2O_3/MCM-41.

with 100 kHz field modulation. The magnetic field was calibrated with a proton resonance meter, and tetracyanoethylene ($g = 2.0077$) as reference. The spectra were recorded at room temperature (300 K) as well as at liquid nitrogen temperature (77 K). Mössbauer spectral measurements were performed in transmission geometry with 2.0 GBq equipped with a ^{57}Co source in a rhodium matrix on a Ranger MS900 spectrometer. Probability distribution of the hyperfine magnetic field was calculated from an experimental Mössbauer spectrum with software developed by G. Le Caer. A Lorenzian function was assumed for the source line shape. The calculation was performed in a hyperfine magnetic field range of 0–60 T intervals. The spectra were recorded with a ranger electronics MS-700MR Mössbauer spectrometer in the temperature range 4–300 K with a speed of -10 to $+10$ mm s^{-1}. The iron content of the samples was determined by ICP-AES on a Labtam Plasm Lab 8440 equipment.

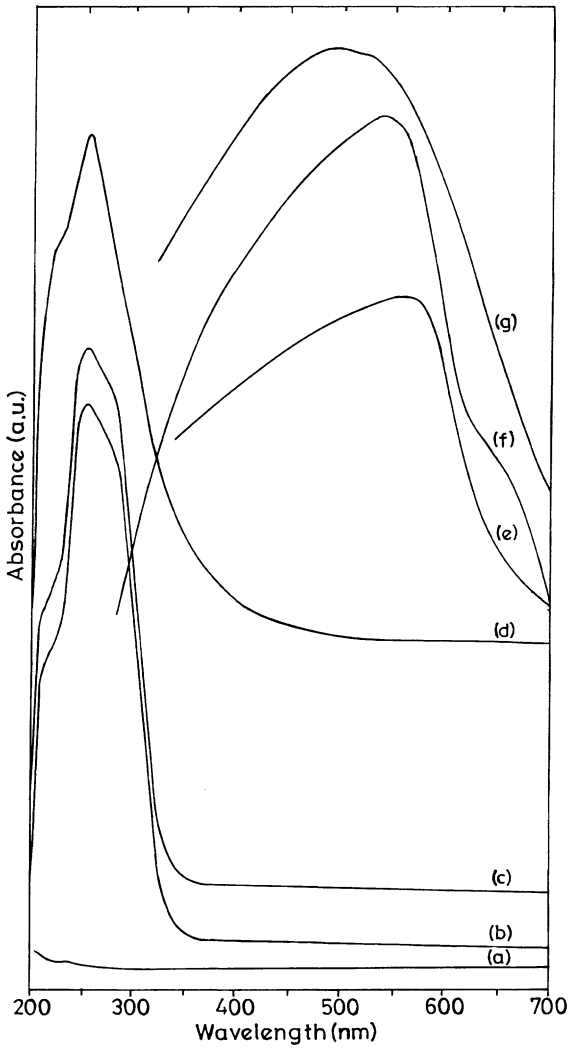

Fig. 2. DRUV–VIS spectra of: (a) calcined MCM-41; (b) FeO(OH)/MCM-41; (c) Fe_2O_3/MCM-41; (d) FeMCM-41; (e) Fe_2O_3; (f) FeO(OH); (g) calcined FeO(OH).

3. Results and discussion

The XRD pattern of FeMCM-41 (not reproduced here) was typical characteristic of mesoporous (hexagonal) MCM-41 structure [12,13]. Fig. 1 shows the

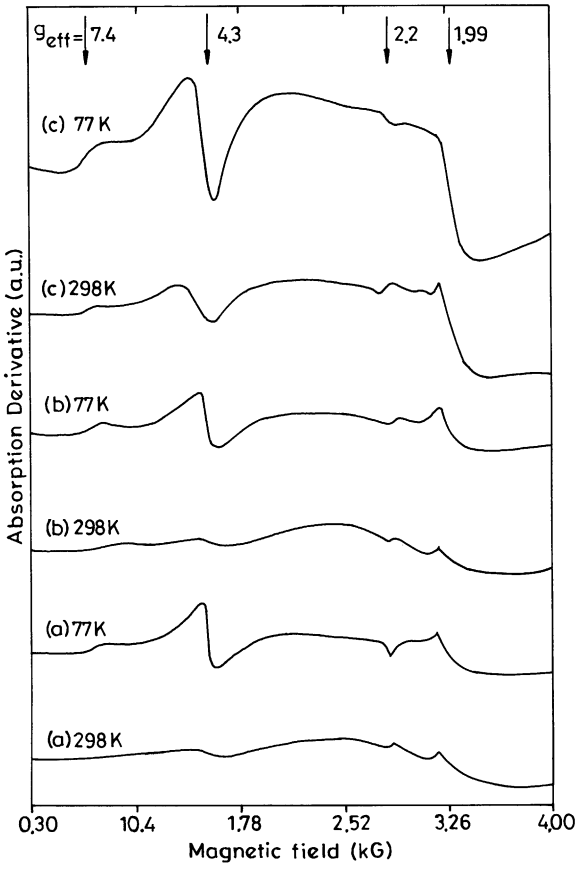

Fig. 3. EPR spectra of: (a) FeO(OH)/MCM-41; (b) Fe_2O_3/MCM-41; (c) FeMCM-41.

diffraction patterns of calcined MCM-41, FeO(OH)/MCM-41 and Fe_2O_3/MCM-41 samples. It is clear from the figure that the loaded samples retain hexagonal MCM-41 structure even after the loading and the subsequent treatments. It is expected that the loaded nanoparticles preferentially reside in the mesopores of MCM-41, and therefore no considerable change is anticipated in the XRD data. However, it is interesting to note that the d_{100}-spacing values of the loaded samples (d_{100} = 38.70 Å for FeO(OH)/MCM-41; d_{100} = 38.71 Å for Fe_2O_3/MCM-41) were increased significantly as compared to the unloaded sample (d_{100} = 36.18 Å for MCM-41). The same holds also for the Fe_2O_3/MCM-48 (d_{211} = 37.80 Å) and MCM-48 (d_{211} = 36.40 Å) [22]. Such an expansion in the unit cell dimension may possibly due to the isomorphous substitution of trivalent iron for the tetravalent silicon in the framework. On this basis, the increase is quite understandable by considering the crystal radii of the ions in tetrahedral geometry ($r_{Si^{4+}}$ = 0.40 and $r_{Fe^{3+}}$ = 0.63 Å) [25]. Recently, a similar expansion in lattice parameter is observed by Bourlinos et al. [26] for Fe(III) exchanged siliceous MCM-41 sample and it is accounted for Fe^{3+} substitution in the silicate framework. The iron contents for FeMCM-41 and Fe_2O_3/MCM-41 samples were 0.8 and 0.7 wt.%, respectively.

The DRUV–VIS spectra (Fig. 2) of loaded samples show absorption band at ~250 nm, whereas the bulk FeO(OH), Fe_2O_3 and calcined FeO(OH), show strong maxima at 535, 560, and 515 nm, respectively [19,20]. However, it is interesting to note that FeMCM-41 also

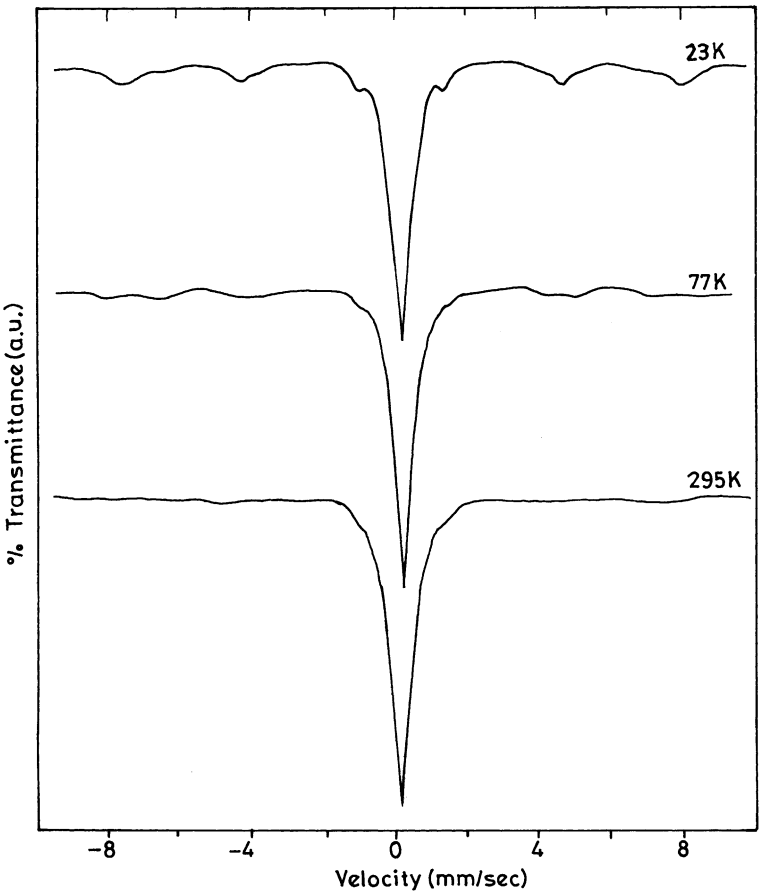

Fig. 4. Mössbauer spectra of Fe_2O_3/MCM-41.

absorbs nearly in the same region (~250 nm) as that of the loaded samples [23,24]. Thus, the occurrence of these absorption bands in this range can be interpreted for both framework trivalent iron and iron oxide nanoparticles (non-framework) inside the mesopores. Hence, due care must be taken in deducing the information regarding the nature of the species on the basis of DRUV–VIS spectra alone. In present DRUV–VIS study, we have not observed the formation of iron oxides particles on the outer surface of MCM-41, unless iron salt concentration (0.01 M) is increased, which gives the absorption in the range of 350–550 nm. Taking into account, the observation of Abe et al. [19,20], we can exclude the possibility of formation of bulk iron oxide particles on the outer surface of MCM-41 in the present report. Fig. 3 presents the EPR spectra of various samples at room as well as liquid nitrogen temperature. Three different signals appeared at various g_{eff} values ~4.30, 2.20 and 1.99 usually observed in iron containing silicate matrix. On the basis of signal assignment [23,24,27–34], the transitions at 4.30 and 1.99 are attributed to trivalent (paramagnetic) iron in the distorted and symmetrical tetrahedral framework sites. The weak signal at 2.1–2.3, which is prominent at 77 K, is assigned to nanosized (superparamagnetic) clusters within the mesopores of MCM-41 [28,29,32]. Thus, it is inferred that during the process of loading, trivalent iron partly substitutes in the silicate framework of MCM-41 with a simultaneous incorporation of nanoparticles in the mesopores.

Fig. 4 shows the Mössbauer spectra of Fe_2O_3/MCM-41 record at different temperatures. The room temperature spectrum shows a sharp singlet with isomer shift ($\delta = 0.3\,mms^{-1}$) and quadrupole splitting ($\Delta < 0.5\,mms^{-1}$) relative to metallic α-iron. This is indicative of high-spin (paramagnetic) Fe^{3+} in the tetrahedral framework sites. This is in agreement with a similar observation in certain mircroporous ferrisilicates [11,29,30] as well as in mesoporous FeMCM-41 [35]. However, upon cooling weak lines (sextet) start to appear at 77 K in addition to the main signal. Further lowering of the temperature down to 23 K results in a clear sextet pattern, which is a characteristic of superparamagentic iron oxides [30]. At this juncture, it is interesting to note that the singlet still remains which is an indicative of the substituted (paramagnetic) Fe(III) in the silicate matrix. Further, it is noteworthy that a reversible effect, viz. the disappearance of the sextet was observed as the temperature increases, which is in agreement with Vertes et al. [36].

4. Conclusion

In summary, various physico-chemical studies on FeO(OH)/MCM-41 and Fe_2O_3/MCM-41 systems showed evidence for the coexistence of paramagnetic and superparamagnetic Fe(III) in the mesoporous matrix. EPR results gave indication for the presence of both type of species in the mesophase. This observation is further supported by Mössbauer data, where they exhibit signature characteristic of paramagnetic and superparamagnetic behaviour. More importantly, the present study warrants the use of DRUV–VIS to derive the information regarding the incorporation of FeO(OH)/Fe_2O_3 nanoparticles in MCM-41. Therefore, extreme care must taken in assigning the DRUV–VIS absorption band of the iron oxide nanoparticles in MCM-41 since the absorption band of the isomorphously substituted Fe(III) in the mesoporous framework, i.e. FeMCM-41, also appears in the same region.

Acknowledgements

We thank Dr. P. Veluchamy (Gifu) for XRD, and RSIC, IIT – Bombay for EPR measurements.

References

[1] M.L. Steigerwald, L.E. Brus, Acc. Chem. Res. 23 (1990) 183.
[2] J.K. Vassiliou, V. Mehtotra, J.W. Otto, N.R. Dollahon, Mater. Sci. Forum 225–227 (1996) 725.
[3] J.H. Fendler, Chem. Mater. 8 (1996) 1616.
[4] X. Zhang, S.A. Jenekhe, H. Perlstein, J. Chem. Mater. 8 (1996) 1571.
[5] C.P. Bean, T.D. Livingston, J. Appl. Phys. 30 (1959) 120.
[6] G.D. Stucky, J.E.M. Dougall, Science 247 (1990) 669.
[7] D.W. Breck, Zeolite Molecular Sieve, Wiley, New York, 1974.
[8] R. Szostak, Molecular Sieves: Principles of Synthesis and Identification, van Nostranel Reinhold, New York, 1989.
[9] C.R. Martin, Acc. Chem. Res. 3 (1991) 457.
[10] J.L. Garcia, A. Loper, F.T. Lazaro, C. Martinez, A. Corma, J. Magn. Magn. Mater. 157/158 (1996) 272.
[11] A. Loper, F.J. Lazaro, J.L. Garcia-Palacios, A. Larrea, Q.A. Pankhurst, C. Martiner, A. Corma, J. Mater. Res. 12 (1997) 1519.

[12] C.T. Kresge, M.E. Leonowicz, W.T. Roth, J.C. Vartuli, J.S. Beck, Nature 359 (1992) 710.
[13] J.S. Beck, J.C. Vartuli, W.J. Roth, M.E. Leonowicz, C.T. Kresge, K.D. Schmitt, C.T.W. Chu, D.H. Olson, E.W. Sheppard, S.B. McCullen, J.B. Higgins, J.L. Schelnker, J. Am. Chem. Soc. 114 (1992) 10834.
[14] X.S. Zhao, G.Q. Lu, G.J. Millar, Ind. Eng. Chem. Res. 35 (1996) 2075.
[15] A. Sayari, Chem. Mater. 8 (1996) 1840.
[16] A. Corma, Chem. Rev. 97 (1997) 2373.
[17] K. Moller, T. Bein, Chem. Mater. 10 (1998) 2950.
[18] P. Selvam, D. Singh, R. Tyagi, S.K. Badamali, V. Ragihi, A.Q. Contractor, in: V. Murugesan, B. Arabindoo, M. Palanichamy (Eds.), Recent Trends in Catalysis Narosa, New Delhi, 1999, p. 550.
[19] T. Abe, Y. Tachibana, T. Uematsu, M. Iwamoto, J. Chem. Soc., Chem. Commun. (1995) 1617.
[20] M. Iwamoto, T. Abe, Y. Tachibana, J. Mol. Catal. A 155 (2000) 143.
[21] M. Fröba, R. Kohn, G. Bouffaud, Chem. Mater. 11 (1999) 2858.
[22] S.K. Badamali, S.E. Dapurkar, S.K. Mohapatra, P. Selvam, in: Proceedings of the 2nd International Symposium on Mesoporous Molecular Sieves, Quebec, 27 August–2 September 2000, p. 146.
[23] S.K. Badamali, P. Selvam, Stud. Surf. Sci. Catal. 113 (1998) 749.
[24] S.K. Badamali, A. Sakthivel, P. Selvam, Catal. Lett. 65 (2000) 153.
[25] R.D. Shannon, Acta Crystallogr. A 32 (1976) 751.
[26] A.B. Bourlinos, M.A. Karakassides, D. Petridis, J. Phys. Chem. 104 (2000) 4375.
[27] T. Castner, G.S. Newell, W.C. Holton, C.P. Slichter, J. Chem. Phys. 32 (1960) 668.
[28] E.G. Derouane, M. Mestdagh, L. Vielvoye, J. Catal. 33 (1974) 169.
[29] D.H. Lin, G. Coudurier, J.C. Vedrine, Stud. Surf. Sci. Catal. 49 (1989) 1431.
[30] S. Schubert, H.M. Ziethen, A.X. Trautwein, F. Schmidt, H.-X. Li, J.A. Martens, P.A. Jacobs, Stud. Surf. Sci. Catal. 46 (1989) 735.
[31] R. Ratnasamy, R. Kumar, Catal. Today 9 (1991) 328.
[32] D. Goldfarb, M. Bernardo, K.G. Strohmaier, D.E.W. Vaughan, H.J. Thomann, J. Am. Chem. Soc. 116 (1994) 6344.
[33] Z.Y. Yuan, S.Q. Liu, T.H. Chen, J.Z. Wang, He.X. Li, J. Chem. Soc., Chem. Commun. (1995) 973.
[34] S. Bordiga, R. Buzzoni, F. Geobaldo, C. Lamberti, T.E. Giamello, A. Zecchina Leofanti, G. Petrini, G. Tozzola, G. Vlaic, J. Catal. 158 (1996) 486.
[35] P. Selvam, S.K. Badamali, M. Murugasen, H. Kuwano, in: V. Murugesan, B. Arabindoo, M. Palanichamy (Eds.), Recent Trends in Catalysis Narosa, New Delhi, 1999, p. 556.
[36] A. Vertes, K. Lazar, K. Kelemen, L. Bogueir, Radiochem. Radioanal. Lett. 4 (1970) 375.